

A Fully Automated Texture-based Approach for the Segmentation of Sequential IVUS Images

M. Papadogiorgaki¹, V. Mezaris¹, Y.S. Chatzizisis², I. Kompatsiaris¹ and G.D. Giannoglou²

¹Informatics and Telematics Institute / Centre for Research and Technology Hellas
1st Km Thermi-Panorama Road, P.O. Box 361, GR-57001 Thermi-Thessaloniki, Greece
Phone: +30 2310 464160 Fax: +30 2310 464164 E-mail: [mpapad, bmezaris, ikom]@iti.gr

²Cardiovascular Engineering and Atherosclerosis Laboratory, AHEPA University Hospital,
Aristotle University Medical School
1st Kyriakidi Str, GR-54636, Thessaloniki, Greece
Phone: +30 2310 994837 Fax: +30 2310 994837 E-mail: [joc, yan]@med.auth.gr

Keywords: coronary arteries, intravascular ultrasound, coronary atherosclerosis, contour initialization, image segmentation, texture analysis.

During the past decade, intravascular ultrasound (IVUS) has become an increasingly important tool in clinical and research applications. The detection of lumen and media-adventitia borders in IVUS images represent a very important procedure for the 3D reconstruction of human coronary arteries, in order to enable reliable quantitative assessment of the atherosclerotic lesions. To serve this goal, a fully automated technique for the detection of lumen and media-adventitia boundaries has been developed. This comprises two different approaches developed for the detection of each boundary based on the results of texture analysis, using a multilevel Discreet Wavelet Frames decomposition. The proposed method shows promising results, indicating the importance of texture features for IVUS image analysis.

1. INTRODUCTION

Coronary angiography is acknowledged as the gold standard for imaging and diagnosis of coronary heart disease. However it is restricted by its inability to depict the vessel wall, provided that it illustrates the coronary arteries as a silhouette of the lumen. Thus, it fails to quantify plaque burden, responsible for partial or total obstruction of the arteries. Recently, intravascular ultrasound (IVUS) has been introduced as a complementary to angiography diagnostic technique aiming to more accurate imaging of coronary atherosclerosis [1].

IVUS is a catheter-based technique that renders two-dimensional images of coronary arteries and therefore, provides accurate information concerning luminal and wall area, plaque morphology and wall composition. However, due to their tomographic nature, isolated IVUS images provide limited information regarding the burden of atherosclerosis. This limitation can be overcome through 3D reconstruction techniques that stack the sequential 2D images in space [2].

In order to manage the 3D reconstruction of a coronary artery, processing of IVUS images is necessary so that the regions of interest can be detected. The coronary artery wall mainly consists of three layers: intima, media and adventitia, while three regions are supposed to be visualized as distinguished fields in an IVUS image, namely the lumen, the vessel wall (consisted by the intima

and the media layers) and the adventitia plus surroundings, as illustrated in Fig.1(a). The above regions are separated by two closed contours: the inner border, which corresponds to the lumen-wall interface, and the outer border representing the boundary between media and adventitia. A reliable and quick detection of these two borders in sequential IVUS images constitutes the basic step towards plaque morphometric analysis and 3D reconstruction of the coronary arteries.

Traditionally, the segmentation of IVUS images is performed manually, which is a time consuming procedure with results affected by the high inter- and intra-user's variability. To overcome these limitations, several approaches for semi-automated segmentation have been proposed in the literature. Sonka et al implemented a knowledge-based graph searching method incorporating a priori knowledge on coronary artery anatomy and a selected region of interest prior to the automatic border detection [3]. Quite a few variations of active contour model have been investigated including the in vivo validation approach of Giannoglou et al [2]. The active contour principles have been used to allow the extraction of the borders in three dimensions after setting an initial contour in Kovalski et al's approach [4]. However, the contour detection fails for low contrast interface regions such as the luminal border where the blood-wall interface in most images corresponds to weak pixel intensity variation. Klingensmith et al use the frequency information to improve the active surface segmentation algorithms after acquiring the radiofrequency (RF) IVUS data, for plaque characterization [8]. For clinical practice the most attractive approaches are the fully automatic ones. A limited number of them has been developed so far, such as the segmentation based on edge contrast [5]; the latter is shown to be an efficient feature for IVUS image analysis, in combination with the gray level distribution. Brusseau et al [6] exploited an automatic method for detecting the endoluminal border based on an active contour that evolves until it optimally separates regions with different statistical properties without using a pre-selected region of interest or initialization of the contour close to its final position. A fuzzy clustering algorithm for adaptive segmentation in IVUS images [9] is investigated by Filho et al. Cardinal et al present a 3D IVUS segmentation applying Rayleigh probability density functions (PDFs) for modeling the pixel gray value distribution of the vessel wall structures [10]. An automated approach based on

deformable models has been reported by Fotiadis et al [7], who employed a Hopfield neural network for the modification and minimization of an energy function as well as a priori vessel geometry knowledge.

This study presents a fully automated method for the segmentation of IVUS images and specifically for the detection of luminal and medial-adventitial boundaries, based on the results of texture analysis performed by means of a multilevel Discrete Wavelet Frames decomposition. The proposed approach does not require manual initialization of the contours and demonstrates the importance of texture features in IVUS image analysis.

The paper is organized as follows: In section 2, image preprocessing is discussed, followed by texture analysis in section 3. In sections 4 and 5 the proposed methods for contour initialization and contour refinement are developed. Clinical implementation is discussed in section 6 and finally, conclusions are drawn in section 7.

2. IMAGE PREPROCESSING

Preprocessing of the image data for the purpose of applying a texture description method consists of two steps: (a) representation of the images in polar coordinates, and (b) removal of catheter-induced artifacts.

Representation of the images in polar coordinates is important for facilitating the description of local image regions in terms of their radial and tangential characteristics. It also facilitates a number of other detections steps, such as contour initialization and the smoothing of the obtained contour. To this end, each of the original IVUS images is transformed to a polar coordinate image where columns and rows correspond to angle and distance from the center of the catheter, respectively, and this image alone, denoted $I(r, \theta)$, is used throughout the analysis process.

The images produced by IVUS include not only tissue and blood regions but also the outer boundary of the catheter itself. The latter defines a dead zone of radius equal to that of the catheter, where no useful information is contained. Knowing the diameter D of the catheter, these catheter-induced artifacts are easily removed by setting $I(r, \theta) = 0$ for $r < D/2 + e$, e being a small constant. This preprocessing is illustrated in Fig 1.

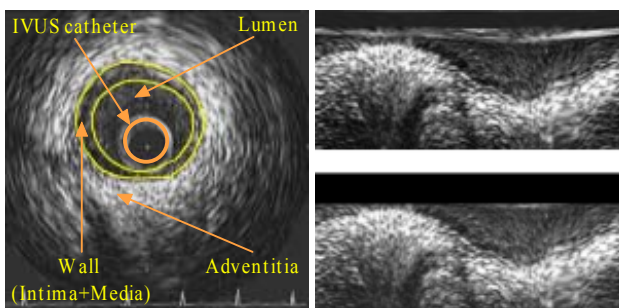


Fig. 1. Original IVUS image (left) and corresponding polar coordinate images before (right top) and after (right bottom) the removal of catheter-induced artifacts.

3. TEXTURE ANALYSIS

Texture has been shown to be an important cue for the analysis of generic images [11]. In this work, the Discrete Wavelet Frames (DWF) decomposition [12] is used for detecting and characterizing texture properties in the neighborhood of each pixel. This is a method similar to the Discrete Wavelet Transform (DWT) that uses a filter bank to decompose the grayscale image to a set of subbands. The main difference between DWT and DWF is that in the latter the output of the filter bank is not subsampled. The DWF approach has been proven to decrease the variability of the estimated texture features, thus improving pixel classification for the purpose of image segmentation. The employed filter bank is based on the lowpass Haar filter

$$H(z) = \frac{1}{2}(1 + z^{-1}) \quad (1)$$

Using this along with the complementary highpass filter $G(z)$, defined as $G(z) = zH(-z^{-1})$, the fast iterative scheme proposed in [12] for applying the DWF analysis in the two-dimensional space is realized as shown in Fig. 2. Then, according to the DWF theory, the texture of pixel \mathbf{p} can be characterized by the standard deviations of all detail components, calculated in a neighborhood F of pixel \mathbf{p} . The calculation of these standard deviations is denoted by the σ blocks in Fig.2. The images resulting from treating each calculated standard deviation as intensity value of pixel \mathbf{p} are denoted as I_k , $k = 1 \dots K$. In the proposed approach, a DWF decomposition of four levels is employed, resulting in $K = 12$ such images, in addition to an approximation component, which is a low-pass filtered image denoted I_{LL} . However, not all of these images are used for the localization of the contours, as discussed in the sequel.

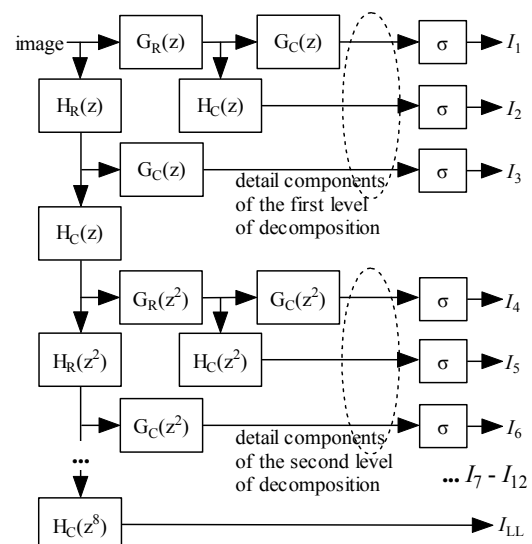


Fig. 2. Fast iterative 2D DWF decomposition of four levels (only the first 2 levels are shown in detail). Subscripts R, C denote filters applied row-wise and column-wise, respectively.

Due to the definition of the filters that are applied for texture analysis, the resulting approximation component of

the filter bank features dominant tangential edges of the input image shifted in the radial direction by a constant number of pixels. This is undesired for the localization of these edges and is resolved by reversely shifting the entire image, $I_{LL}(r, \theta) = I_{LL,orig}(r + c, \theta)$, by a constant c .

4. CONTOUR INITIALIZATION

Objective of the contour initialization procedure is the detection of pixels that are likely to belong to the lumen and media-adventitia boundaries, taking into consideration the previously extracted texture features.

Let I_{int} , I_{ext} denote the simplified images, after texture analysis, which are used for detecting the lumen and media-adventitia boundaries respectively. These are defined under the proposed approach as

$$I_{int}(r, \theta) = \frac{255}{\max_{(r, \theta)} \{I'_{int}(r, \theta)\}} I'_{int}(r, \theta), \quad (2)$$

$$I_{int}(r, \theta) = \sum_{k=\{7,8,10,11\}} I_k(r, \theta) \\ I_{ext}(r, \theta) \equiv I_{LL}(r, \theta) \quad (3)$$

The choice of the images I_k that are employed in this initialization process was done heuristically, based on visual evaluation of all K generated images.

The internal contour is initialized as the set of pixels

$$c_{int} = \{\mathbf{p}_{int} = [\rho, \theta]\} \quad (4)$$

for which

$$I_{int}(\rho, \theta) > T \text{ and } I_{int}(r, \theta) < T \quad \forall r < \rho$$

thus defining an internal contour function $C_{int}(\theta) = \rho$.

The external contour is initialized as the set of pixels

$$c_{ext} = \{\mathbf{p}_{ext} = [\mu, \theta]\} \quad (5)$$

for which

$$I_{ext}(\mu, \theta) = \max_{r > \rho'} \{I_{ext}(r, \theta)\},$$

where $[\rho', \theta]$ are the points of the final internal contour, as obtained by applying to the initialization data the refinement process of the following section. This defines an external contour function $C_{ext}(\theta) = \mu$.

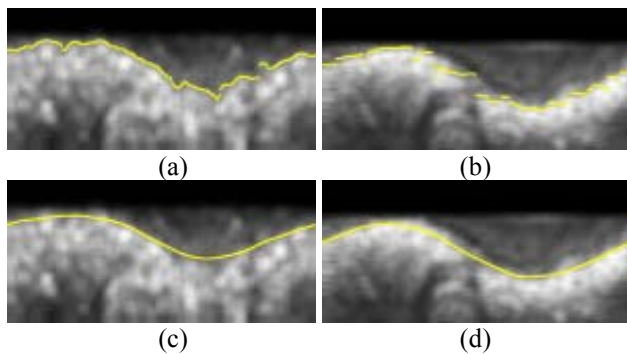


Fig. 3. Results of contour initialization for (a) the lumen, (b) the media-adventitia boundary, and (c), (d) the corresponding contours after low pass filtering-based contour refinement.

The motivation behind the choice of the approximation component of the DWF decomposition for the

initialization of the media-adventitia boundary lies in the observation that the latter is represented by a thick bright ring (a thick bright curve in polar coordinates) that is dominant in the image. Thus, in the approximation component, the media-adventitia boundary is well preserved, as opposed to higher-frequency details that are suppressed by the low-pass filtering, facilitating contour initialization.

5. CONTOUR REFINEMENT

In contrast to the initial contours generated as described in the previous section, which are not smooth and are characterized by discontinuities, the true lumen and media-adventitia boundaries are smooth, continuous functions of θ . Consequently, in order to obtain smooth contours that are consistent with the true ones, the application of a filtering or approximation procedure to the initial contour functions $C_{int}(\theta)$, $C_{ext}(\theta)$ is required.

In this work, a simple low-pass filtering solution is adopted that takes advantage of the filtering functionalities developed for the purpose of texture analysis. More specifically, the low-pass filters $H(z^{2^i})$, $i = 0, \dots, M-1$ that are based on the low pass Haar filter (Eq. 1) are successively applied to each of the two initial contour functions. This process is illustrated in Fig. 4. This simple procedure is shown to perform acceptably in smoothing the contours; however, better results can probably be obtained using a more elaborate approximation technique such as one based on radial basis functions.

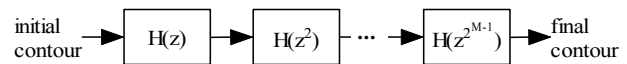


Fig. 4. Illustration of the low-pass filtering-based contour smoothing procedure.

6. CLINICAL IMPLEMENTATION

The developed IVUS image analysis methodology was applied to a set of 57 images. These were captures using a mechanical imaging system [2] and a 2.6F sheath-based catheter, incorporating a 40 MHz single-element transducer rotating at 1800 rpm and generating 30 images/sec. A motorized pullback device was used to draw out the catheter at a constant speed of 0.5 mm/sec. The ultrasound data was recorded in a 0.5-inch S-VHS videotape. The S-VHS data was digitized by an integrated to the IVUS console frame grabber at 512x512 pixels with 8-bit grey scale in a rate of 7.5 images/sec and the end-diastolic images were selected (peak of R-wave on ECG). The selected digitized images constituted the experimentation dataset of the proposed analysis approach.

Indicative results of the proposed approach are presented in Fig. 5 (on the right column), where the boundaries manually detected by a domain expert are also shown (on the left column). The presented results demonstrate the promising performance of the developed method and, most importantly, highlight the suitability and significance of the texture features employed under the proposed approach.

7. CONCLUSIONS

In this paper an automated approach for the detection of lumen and media-adventitia boundaries in IVUS images has been presented, based on the results of texture analysis. The proposed approach does not require manual initialization of the contours. The experiments conducted by applying the developed technique to real data showed promising results and demonstrated the usefulness of the employed texture features for IVUS image analysis. Future developments of this work include the combination of the texture features with other features reported in the related literature for contour initialization and the introduction of improved contour approximation techniques.

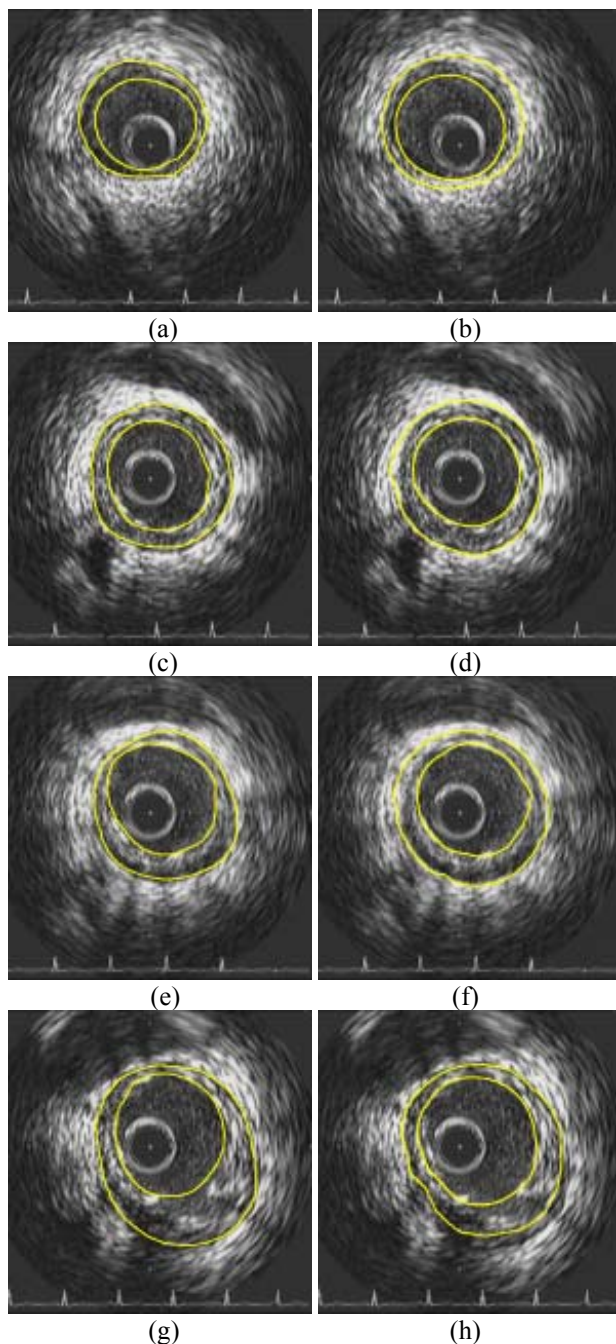


Fig. 5. Experimental results for different images of the proposed approach in (b), (d), (f), (h) and comparison with corresponding contours manually generated by experts in (a), (c), (e), (g) accordingly.

ACKNOWLEDGMENT

The work presented in this paper was partially supported by the Hungary-Greece bilateral cooperation "CIRCE", COST 292, the Greek State Scholarships Foundation and the Aristotle University Research Committee.

REFERENCES

- [1] C. Di Mario, G. Gorge, et al, "Clinical application and image interpretation in intracoronary ultrasound", *European Heart Journal*, vol. 19, p. 207-229, 1998.
- [2] G.D. Giannoglou, Y.S. Chatzizisis, et al, "In Vivo Validation of an Active Contour Model for Segmentation of Sequential Intravascular Ultrasound Images", *Computers in Biology and Medicine*, under review.
- [3] M. Sonka, X. Zhang, et al, "Segmentation of intravascular ultrasound images: A knowledge-based approach", *IEEE Trans. on Medical Imaging*, vol. 14, p. 719-732, 1995.
- [4] G. Kovalski, R. Beyar, et al, "Three-dimensional automatic quantitative analysis of intravascular ultrasound images", *Ultrasound in Med. & Biol.*, vol. 26, p. 527-537, 2000.
- [5] H. Zhu, Y. Liang, M.H. Friedman, "IVUS image segmentation based on contrast", *Processing of SPIE*, Durham, NC, USA, 4684: 1727-1733, 2002.
- [6] E. Brusseau, C.L. de Korte, et al, "Fully automatic luminal contour segmentation in intracoronary ultrasound imaging - A statistical approach", *IEEE Trans. on Med. Imaging*, vol. 23 p. 554-566, 2004.
- [7] M.E. Plissiti, D.I. Fotiadis, et al, "An Automated Method for Lumen and Media-Adventitia Border Detection in a Sequence of IVUS Frames", *IEEE Trans. on information technology in Biomedicine*, vol. 8, no. 2, 2004.
- [8] J.D. Klingensmith, A. Nair, et al, "Segmentation of three-dimensional intravascular ultrasound images using spectral analysis and a dual active surface model", *2004 IEEE Ultrasonics Symposium*, vol. 3, p. 1765 - 1768, 2004.
- [9] E. dos S. Filho, M. Yoshizawa, et al, "Detection of Luminal Contour Using Fuzzy Clustering and Mathematical Morphology in Intravascular Ultrasound Images", *2005 IEEE-EMBS Engineering in Medicine and Biology Society, 27th Annual International Conference*, p. 3471 - 3474, 2005.
- [10] M.-H.R. Cardinal, J. Meunier, et al, "Intravascular Ultrasound Image Segmentation: A Three-Dimensional Fast-Marching Method Based on Gray Level Distributions", *IEEE Trans. on Medical Imaging*, vol 25, p. 590 - 601, 2006.
- [11] V. Mezaris, I. Kompatsiaris and M. G. Strintzis, "Still Image Segmentation Tools for Object-based Multimedia Applications", *International Journal of Pattern Recognition and Artificial Intelligence*, vol. 18, no. 4, p. 701-725, 2004.
- [12] M. Unser, "Texture classification and segmentation using wavelet frames", *IEEE Transactions on Image Processing*, vol. 4, no. 11, p. 1549-1560, 1995.